Atmos. Chem. Phys. Discuss., 8, 17939–17986, 2008
www.atmos-chem-phys-discuss.net/8/17939/2008/

Atmospheric Chemistry and Physics Discussions

This discussion paper is/has been under review for the journal *Atmospheric Chemistry and Physics (ACP)*. Please refer to the corresponding final paper in *ACP* if available.

Exploring the relation between aerosol optical depth and $PM_{2.5}$ at Cabauw, the Netherlands

M. Schaap[1], A. Apituley[2], R. M. A. Timmermans[1], R. B. A. Koelemeijer[3], and G. de Leeuw[1,4,5]

[1]TNO, Business unit Environment, Health and Safety, P.O. Box 80015, 3508 TA Utrecht, The Netherlands
[2]National Institute for Public Health and the Environment, P.O. Box 1, 3720 AH Bilthoven, The Netherlands
[3]Netherlands Environmental Assessment Agency (MNP), P.O. Box 303, 3720 AH Bilthoven, The Netherlands
[4]Finnish Meteorological Institute, Climate Change Unit, P.O. Box 503, 00101 Helsinki, Finland
[5]University of Helsinki, Department of Physics, P.O. Box 64, 00014 Helsinki, Finland

Received: 18 July 2008 – Accepted: 25 August 2008 – Published: 2 October 2008

Correspondence to: M. Schaap (martijn.schaap@tno.nl)

Published by Copernicus Publications on behalf of the European Geosciences Union.

Abstract

To acquire daily estimates of $PM_{2.5}$ distributions based on satellite data one depends critically on an established relation between AOD and ground level $PM_{2.5}$. In this study we aimed to experimentally establish the AOD-$PM_{2.5}$ relationship for the Netherlands. For that purpose an experiment was set-up at the AERONET site Cabauw. The average $PM_{2.5}$ concentration during this ten month study was 18 μg/m^3, which confirms that the Netherlands are characterised by a high PM burden.

A first inspection of the AERONET level 1.5 (L1.5) AOD and $PM_{2.5}$ data at Cabauw showed a low correlation between the two properties. However, after screening for cloud contamination in the AERONET L1.5 data, the correlation improved substantially. When also constraining the dataset to data points acquired around noon, the correlation between AOD and $PM_{2.5}$ amounted to R^2=0.6 for situations with fair weather. This indicates that AOD data contain information about the temporal evolution of $PM_{2.5}$. We had used LIDAR observations to detect residual cloud contamination in the AERONET L1.5 data. Comparison of our cloud-screed L1.5 with AERONET L2 data that became available near the end of the study showed favorable agreement.

The final relation found for Cabauw is $PM_{2.5}$=124.5*AOD–0.34 (with $PM_{2.5}$ in μg/m^3) and is valid for fair weather conditions. The relationship determined between MODIS AOD and ground level $PM_{2.5}$ at Cabauw is very similar to that based on the much larger dataset from the sun photometer data, after correcting for a systematic overestimation of the MODIS data of 0.05. We applied the relationship to a MODIS composite map to assess the $PM_{2.5}$ distribution over the Netherlands. Spatial dependent systematic errors in the MODIS AOD, probably related to variability in surface reflectance, hamper a meaningful analysis of the spatial distribution of $PM_{2.5}$ using AOD data at the scale of the Netherlands.

ACPD

8, 17939–17986, 2008

1 Introduction

While air quality in Europe has improved substantially over the past decades, air pollution still poses a significant threat to human health (EEA, 2007). Health effects of air pollution are dominated by particulate matter, both $PM_{2.5}$ and PM_{10}. Short-term exposure to PM_x has frequently been associated with increased human morbidity and mortality (e.g. Brunekreef and Holgate, 2002). Effects of long-term exposure to PM are much more uncertain than the short-term effects, but are believed to have a much greater effect on health loss (Dockery et al., 1993; Pope et al., 1995; Kappos et al., 2004). For the assessment of the exposure to particulate matter the determination of the aerosol mass and its composition is mandatory. Traditionally, in situ observations are used to derive information on the large scale features of air pollutants. In case of particulate matter this approach is hampered by the difficulties in the sampling techniques and the highly variable concentrations in space and time. Satellite remote sensing may be a cost-effective method to monitor the highly variable aerosol fields on regional scales.

Satellite measurements provide full spatial coverage and are – in principle – consistent for the whole European region. However, they are less precise than in-situ observations. This suggests that satellite measurements may be useful to improve the insight in regional PM distributions in combination with models and ground based measurements. For Europe, a PM_{10} distribution has been derived using geo-statistical techniques combining in-situ observations, modelled distributions and MODIS (MODerate-resolution Imaging Spectroradiometer) satellite data (van de Kasteele et al., 2006). The authors showed that the use of both model and remote sensed data improved the quality of the estimated annual average PM_{10} distribution. Several studies have used empirical relations between AOD and $PM_{2.5}$ or PM_{10} to estimate the PM distributions over larger regions (e.g. Kacenelenbogen et al., 2006; Vidot et al., 2008). Van Donkelaar et al. (2006) calculated the relation between AOD and ground level $PM_{2.5}$ with a model and multiplied this with the retrieved AOD to arrive at an estimate for the ambient $PM_{2.5}$ level on a global scale. Furthermore, the advent of satellite observations has also led to a development of data assimilation schemes that assimilate aerosol optical thickness directly into models (e.g. Builtjes et al., 2001; Collins et al., 2001; Koelemeijer et al., 2006a). In the latter approaches the (modelled) relation between AOD and $PM_{2.5}$ is an uncertain and limiting factor in determining the absolute $PM_{2.5}$ concentrations from satellite data. Strong correlations and an improved understanding of this relation are needed to generate reliable satellite derived estimates of the particulate matter distribution in a region.

Various studies have reported empirical relations between AOD and PM_{10} or $PM_{2.5}$ measurements for different parts of the world (e.g. Wang and Christopher, 2003; Hutchison, 2003; Chu et al., 2003; Engel-Cox et al., 2004, 2006; Al-Saadi et al., 2005; Kacenelenbogen et al., 2006; Koelemeijer et al., 2006b; Kumar et al., 2007; Liu et al., 2007; Gupta and Christopher, 2007; Mukai et al., 2008). For example, promising correlations are found between time-series of AOD and $PM_{2.5}$ for many stations in the Eastern and Midwest US. Other stations, however, particularly in the Western US, show hardly any correlation (Wang and Christopher, 2003; Hutchison, 2003; Engel-Cox et al., 2004). Variations in local meteorological conditions, occurrence of multiple aerosol layers, and variations in aerosol chemical composition likely play an important role in determining the strengths of such correlations. For example, Koelemeijer et al. (2006b) showed that the correlation between PM and AOD is improved when the AOD is divided by the mixing layer height and, to a lesser extent, when it is corrected for growth of aerosols with relative humidity.

To acquire daily estimates of $PM_{2.5}$ distributions one depends critically on an established relation between AOD and ground level $PM_{2.5}$. In this study we aimed to experimentally establish this relationship for the Netherlands. For this purpose a field study was conducted at the Cabauw Experimental Site for Atmospheric Research – CESAR (Sect. 2). We combine $PM_{2.5}$ measurements with sun photometer data to empirically determine the AOD-$PM_{2.5}$ relationship (Sect. 3). In Sect. 4 we explore the usefulness of the obtained relationship for mapping $PM_{2.5}$ over the Netherlands using

MODIS AOD. Finally, we present an extensive discussion of our results in comparison to the literature in Sect. 5.

2 Methodology

2.1 Experimental setup

To address the relation between AOD and $PM_{2.5}$ a study was set-up to monitor $PM_{2.5}$ between the 1 August 2006 and 31 May 2007, at the Cabauw Experimental Site for Atmospheric Research (CESAR). CESAR (Russchenberg et al., 2005; http://www.cesar-observatory.nl) is the focal point of experimental atmospheric research in The Netherlands. The site is located in a rural area in the central part of Netherlands (51.97° N, 4.93° E) and hosts a comprehensive set of active and passive remote sensing instruments, as well as in-situ observations. The combination of the instrumentation at Cabauw provides a unique opportunity to study the AOD-$PM_{2.5}$ relationship in the Netherlands.

The aerosol optical depth is routinely monitored using a CIMEL sun photometer and the data are reported to the AERONET (http://aeronet.gsfc.nasa.gov) (Holben et al., 2001). The technical details of the instrument are described in the CIMEL Sun Photometer Manual (http://aeronet.gsfc.nasa.gov). This specific instrument measures the aerosol optical depth at four wavelengths (440 nm, 670 nm, 870 nm and 1020 nm), and the sky radiance in aerosol channels in the azimuth plane (the almucantar technique) and in the principal plane. These data are used in the AERONET standard procedures to retrieve information on columnar aerosol characteristics such as the aerosol optical depth, Angström coefficient and size information. Data processing, cloud-screening algorithm, and inversion techniques are described by Holben et al. (1998, 2001), Eck et al. (1999), Smirnov et al. (2000), Dubovik and King (2000), and Dubovik et al. (2000). We have used the Level 1.5 (Automatically cloud cleared) AOD data in this study. The Level 2 data (Pre- and post-field calibration applied, automatically cloud cleared and

ACPD
8, 17939–17986, 2008

manually inspected) are updated on a yearly basis and were only available for part of campaign and will be used for a sensitivity study.

We installed a Tapered Element Oscillating Microbalance with Filter Dynamics Measurement System (TEOM-FDMS) to monitor the ambient $PM_{2.5}$ concentrations. A standard TEOM is well known for its underestimation of ambient PM concentrations due to evaporation of semi-volatile components from the microbalance that is conditioned at higher than ambient temperatures. Especially, ammonium nitrate is sensitive to evaporation under these operation conditions. As ammonium nitrate levels are high in the Netherlands (Schaap et al., 2002), we chose to use the TEOM-FDMS instrument, which uses two microbalances in an alternating measurement cycle. At one microbalance the mass increase by sampling ambient air is measured, whereas at the second microbalance the evaporation loss is estimated by sampling particle free air. Evaporation loss is thus unambiguously measured and accounted for in the final measurement result. The role of each microbalance is alternated to keep the loading on both balances representative for each other. Comparison with reference methods shows a general good agreement (Grover et al., 2005). Hence, by using the TEOM-FDMS we obtain estimates of $PM_{2.5}$ inline with the reference method, but with a temporal resolution of half an hour.

Besides these core instruments a range of optical and physical aerosol parameters such as size distribution and aerosol extinction and absorption coefficient are routinely monitored at Cabauw. In this study we have extensively used the RIVM aerosol back scatter LIDAR (Apituley et al., 2000). This instrument provides information on the vertical structure of the aerosol profile, atmospheric layering and the presence of clouds up to 15 km at a temporal resolution of 5 min. The backscatter LIDAR operates at a single wavelength (1064 nm) and is therefore limited it its ability to estimate aerosol optical properties in addition to the qualitative vertical aerosol profile.

2.2 Detection of clouds and mixing layer height

We have used the LIDAR profiles for the detection of the presence of clouds above Cabauw. LIDAR systems can be used to detect clouds as they provide strong scattering peaks in LIDAR data. Moreover, clouds appear as strong modulations in the LIDAR signal with range. We have used a combination of three algorithms to detect clouds based on these characteristics. The first approach is a threshold method where the range corrected LIDAR signals above a threshold are designated as clouds. This works well for high signal to noise ratios (i.e. low clouds). Favourable results are also obtained in noisy cases when smoothing is applied. The latter has the disadvantage of reducing (vertical) resolution. For our study this is not a problem as we are primarily interested in cloud indicators and the cloud height information is of secondary importance. The second algorithm aims to detect strong modulations in the LIDAR signal due to clouds and uses the first order range-derivative as described by Pal et al. (1992). The derivative filter may be set at variable resolution with altitude, so as to enhance detection of high cirrus under noisy conditions. The abovementioned methods only use qualitative signal features. The third, quantitative, method is based on retrieval of the backscatter profile from the LIDAR data (Klett, 1985) and setting a threshold at the scattering level of clouds. All three techniques were applied to the data from the RIVM backscatter LIDAR and a combined approach was used to obtain the best possible reliability at higher altitudes. Based on 5-min sampling time of the LIDAR data, maximally 12 occurrences of clouds can be detected in an hour. Here we require a minimum of 3 cloud detections (out of a maximum of 12 occurrences) to classify the hour as cloudy. This minimum of 3 was chosen to avoid misclassifications induced by noise in the LIDAR signal.

A sun photometer obtains AOD data from measurements looking directly at the sun. The Cabauw LIDAR provides stationary vertical aerosol profiles and cloud detection for a small footprint in the zenith sky only. As it is not un-imaginable that under some circumstances the sun photometer is observing a clear sky under a slant path, while at the same time the LIDAR observes a cloud directly overhead, or vice versa, additional cloud indicators may be needed, for instance, one that provides an estimate of all-sky cloud cover, rather than cloud cover right above the instruments only. For this reason we also investigated the applicability of APCADA (Automatic Partial Cloud Amount Detection Algorithm) technique (Dürr and Philipona, 2004), which has been implemented at the Cabauw site. APCADA provides cloud cover estimates every 10 min during daytime and night-time without distinction in cloud type (altitude). APCADA detects only clouds that have a measurable effect on long-wave downwelling radiation (LDR). Hence, the APCADA algorithm limited sensitivity for high (i.e. cold) clouds.

The mixing layer height can be inferred from backscatter LIDAR or ceilometer data, since aerosol concentrations are often higher within the mixing layer compared to layers above it and can be located at the transition from high-to-low aerosol loading. For the Netherlands the mixing layer height (MLH) is retrieved operationally from LD40 ceilometers as described by de Haij et al. (2007). Unfortunately, the ceilometer at Cabauw was not operational for most of our sampling period. Therefore, we have used the MLH data from the site of de Bilt, about 25 km North-East of the Cabauw station.

2.3 Data handling

The sun photometer AOD data were obtained from the AERONET site to comply with AERONET standards. The TEOM-FDMS provides the $PM_{2.5}$ mass in combination with instrument diagnostics. The instrument provides a range of status codes indicating instrument health and data reliability. We have used only data without a reported malfunction or warning code (status code is 0). Furthermore, we require the concentration to be positive and we disregard all data with a positive correction for the volatile fraction. This screening may be too strict, but it refines the selected data to the best available. From the LIDAR data quicklook plots were drawn for each day for visual inspection of the atmospheric conditions (cloudiness, aerosol layers). In addition, the cloud detection scheme was run for each profile. Standard meteorological variables (T, RH, Wind direction and speed) for the site of Cabauw were taken from the CESAR data portal. A classification of the synoptic situation was obtained from the German Weather Service (Hess and Brezowsky, 1977). All instruments have their own temporal resolution, ranging from minutes to an hour. Hence, for all instruments and the meteorological variables we have computed hourly mean values. Daily data, such as the type of synoptic situation, were assigned to all hours in the concerning day. All data were combined in a single database for use in the analysis.

2.4 MODIS satellite data

The first MODIS instrument was launched onboard the EOS-Terra satellite in December 1999. In May 2002, a second MODIS instrument was launched on board EOS-Aqua. The MODIS instruments measure sunlight reflected by the Earth's atmosphere and surface as well as emitted thermal radiation at 36 wavelengths. At least two observations of any place in Europe are obtained per day during daylight hours because the Terra and Aqua satellites cross Europe near 10:30 and 13:30 local solar time, respectively. The AOD algorithms for application over land and sea surfaces are mutually independent as the radiative properties of water and land are very different. The retrieval is more accurate over ocean than over land because the reflection by water is relatively low outside the region of direct sun glint, algae blooms and suspended matter, and can be computed accurately from the sea surface wind field. The accuracy of MODIS AOD over land is 0.05±15% (Levy et al., 2007a).

The MODIS retrieval (v5) of the AOD over land employs primarily three spectral channels centred at 0.47, 0.66, and 2.1 μm. AOD is derived at 0.47 and 0.66 μm, and interpolated to 0.55 μm. The AOD is only retrieved for cloud-free pixels in a 20×20 pixel area at 500 m resolution and reported at 10×10 km^2 resolution. Only when more than 12 pixels are classified as cloud-free retrieval is attempted. The AOD is retrieved over surfaces that are not highly reflective (hence snow or ice covered surfaces and deserts are excluded). The basics of the algorithms are described in Kaufman and Tanre (1998) and Remer et al. (2005). Recently, a new collection (5) of the AOD data was released. The new MODIS algorithm (v5.2; Levy et al., 2007a,b) has been updated rigorously. The major changes incorporate the new surface reflectivity assumptions, a new set of aerosol model optical properties derived empirically from AERONET, a new aerosol lookup table and a more elaborate inversion scheme. The cloud screening procedure was not changed. As a consequence of all the improvements the new product generally yields significantly lower AOD than the previous collection. A preliminary evaluation shows better agreement with AERONET (Levy et al., 2007a). However, the data from the new collection still need to be evaluated in detail for Europe. A full evaluation is outside the scope of the present project. However, we will evaluate the data for the situation of Cabauw. The MODIS AOD product was mapped on a grid over north-western Europe with a spatial resolution of 0.125×0.0625° lon-lat, which refers to about 10×10 km^2.

3 Results and preliminary discussion

3.1 Time series of AOD and $PM_{2.5}$

A statistical overview of the measured data is presented in Table 1. The average measured AOD was 0.29. The observed AOD values range from virtually zero (0.04) to 2.5, with a median value of 0.25. For Cabauw a longer record of AOD exists as it is part of the AERONET network since 2003. The observed AOD in this study is slightly higher than the average value of 0.26 for the period April 2003 until April 2007, which is probably due to the use of level 1.5 data as discussed below. The measured average $PM_{2.5}$ concentration was 18.2 $\mu g/m^3$. This level is high in comparison to other areas in Europe (Putaud et al., 2004) and confirms that the Netherlands are characterised by a high PM burden. Maximum concentrations were observed during the last days of March and the beginning of April, with a peak value of 156 $\mu g/m^3$.

As a first assessment we have plotted all AOD data against the co-located $PM_{2.5}$ data in a scatter diagram (Fig. 1). At a first glance, there seems to be a large variability and no indication for a well defined relation between the variables. The majority of the data have AOD values lower than 1 and $PM_{2.5}$ concentrations below 100 $\mu g/m^3$. Only ten

ACPD
8, 17939–17986, 2008

data points are outside this area. Some of these data points are clear outliers. On the other hand, four points are associated with the episode of peak $PM_{2.5}$ loads during 29 and 30 March. Although we do not know the reason for the different behaviour during this period, we suspect that large uncertainties may be associated with both AOD and the $PM_{2.5}$ data under these particular circumstances. Hence, we chose to exclude these ten data points from this analysis as they negatively impact the comparability of the analyses presented below. Investigation on instrument properties during peak loads (that do not occur frequently) is still ongoing. A fit through all remaining data learns that only 13% of the variability in $PM_{2.5}$ is explained by AOD.

In Fig. 2 we show the complete time series of AOD and $PM_{2.5}$. $PM_{2.5}$ is given as a grey line and the AOD data are superimposed as diamonds. Visual inspection of the time series for August–September (upper panel) yields a more differentiated picture than the scatter diagram. During August $PM_{2.5}$ concentrations were relatively low, whereas the sun photometer yields high AOD data. The two measures are virtually uncorrelated during this month. In contrast, the AOD and $PM_{2.5}$ data for September track each other very well (R^2=0.65). Inspection for the remainder of the study period confirms that periods with and without correlation follow upon each other. Besides September, a very promising correlation between AOD and $PM_{2.5}$ is found for an extended period between 15 March and 15 May (R^2=0.56).

The data for September and springtime illustrate the potential to define situations in which the AOD may be used to estimate $PM_{2.5}$ levels. However, the periods with high AOD and low $PM_{2.5}$ obscure the statistical analysis. It has been posed in the literature (e.g. de Mey et al., 2007) that sun photometer data may be subject to cloud contamination. Especially cirrus can be optically thin and therefore indistinguishable from aerosol optical depth unless cirrus is detected by independent means. We tested this hypothesis using the lidar data. In Fig. 3 we present time-height lidar plots for two days with high AOD and low $PM_{2.5}$. The colour scale (in arbitrary units) is representative for the light scattering that occurs at a given height at a given point in time. Dark and light blue hues indicate low scattering, green and brown are indicative for aerosols and white is associated with very strongly scattering particles and clouds. The data for 23 August 2006, indicate that variable clouds were present at different heights. The data for 20 September 2006, shows a typical day with fair weather without low clouds. However, optically thin cirrus clouds are present between approximately 06:00 and 12:00 UTC. For both examples AERONET level 1.5 observations were included in the database for several instances during which the LIDAR unambiguously detects clouds. For these examples, the AOD to $PM_{2.5}$ ratio is higher than average. Hence, we concluded that the presence of clouds indeed contaminates the sun photometer AOD measurements. Although we already expected this to be the case with hard to detect cirrus, cloud contamination with broken low-level clouds was not expected. Hence, our next step was to rigorously screen the available $PM_{2.5}$ collocated AERONET data for possible cloud contamination.

3.2 Cloud screened data

In this section we evaluate the impact of the additional quality screening of the AERONET L1.5 data by using APCADA and our LIDAR based methodology.

We show the impact of the additional cloud screening in Fig. 2 for the LIDAR based cloud screening. The AOD data points that passed the additional test are shown as black diamonds, whereas the data points that failed the tests are indicated as open diamonds. A significant portion of the data does not pass the additional test. For example, almost all data points in August, which was identified as a period without any correlation between AOD and $PM_{2.5}$, do not pass the tests and are suspected of being cloud contaminated. Also, single excursions with high AOD, e.g. 16 February, are identified. The data for September, the first period to show a good correlation between our variables, mostly pass the tests. On the other hand, during spring there are a number of situations where data do not pass the test, although the correlation between AOD and $PM_{2.5}$ is obvious. In these cases the cloud screening may be too strict, or the optical thickness of the cloud is very low. However, it is mostly the combinations of low $PM_{2.5}$ and high AOD that are filtered out using these additional analyses.

In Fig. 4 and Table 2 we compare the impact of the two cloud detection approaches on the explained variability between AOD and $PM_{2.5}$. An unexpectedly large number of data points (~50%) was rejected from the AERONET L1.5 data due to both broken cloud conditions and optically thin high cirrus clouds. Both screening methodologies lower the number of combinations with high AOD and low PM concentrations, therewith lowering mean and median AOD values of the remaining data set. The correlation coefficients for the AOD-$PM_{2.5}$ relations after applying the cloud screening are R^2=0.41 (LIDAR) and R^2=0.33 (ACPADA), which is substantially higher than before their application. The screening based on ACPADA is less strict and yields a slightly lower explained variability than the LIDAR based approach. A reason might be that the APCADA algorithm is not very sensitive for high (cirrus) clouds. Consequently, we have used the LIDAR screened AOD data for further analysis.

3.3 Verification of cloud screening using L2.0 data

AERONET level 2.0 data are produced once a year as it requires the calibration of the instrument and a visual inspection of the data by an expert. Prior to manuscript submission, L2.0 data were released for Cabauw for the period until 12 April 2007. These data provide the opportunity to investigate the consequences of using the L1.5 instead of L2.0 data.

The number of valid data points in L2.0 is reduced by about 20% compared to L1.5. The data that are retained in L2.0 are for 98% exactly the same data as in L1.5. The other 2% of the data contains a lower AOD value in L2.0 than in L1.5. The average AOD is reduced from 0.29 in L1.5 to 0.25 in L2.0. The data reduction by one fifth indicates that the cloud screening applied in our study is more strict than that in the final AERONET processing.

In Fig. 5 we have plotted the $PM_{2.5}$ against AOD for L1.5 and L2.0. The grey diamonds represent all available data. Comparison between the versions learns that in L2.0 AOD values above 0.5 which are associated with low $PM_{2.5}$ data have been eliminated. As a consequence, the fit between AOD and $PM_{2.5}$ using all data explain a higher percentage of the variability than in L1.5. The black diamonds represent the data after performing the LIDAR based cloud screening. The close agreement between the two datasets after cloud screening is remarkable. It means that most AOD data points that are excluded in the final AERONET processing from L1.5 to L2.0 are also excluded by our cloud screening. This was confirmed by identifying the data reduction as function of the number of cloud counts per hour (see Table 4). The data reduction in L2.0 is about 10% for the hours with a low number of cloud counts, but increases with cloud count, and sharply increases above nine cloud detections per hour. As our cloud count limit is 3 the screened L1.5 data set is for 90% the same as we would have used based on L2.0 data. The consistency between the data provides confidence in the use of the lidar as an independent and strict method to assess the quality of the sun photometer data. Also, combining L1.5 and collocated lidar observations permit ongoing determination of the AOD-$PM_{2.5}$ relationship without having to wait for the L2 data product.

3.4 Determination of the AOD-$PM_{2.5}$ relationship

The best estimate of the AOD-$PM_{2.5}$ relation is that obtained after cloud screening which resulted in the following linear fit (with $PM_{2.5}$ in μg/m^3):

$PM_{2.5}$=97.5*AOD+2.9 R^2=0.40

Here, we investigate the impact of meteorological conditions and the time of the day on the relation.

3.4.1 Incorporation of mixing layer height

The aerosol optical depth depends on the total vertical aerosol burden, while $PM_{2.5}$ only depends on aerosol concentration near the surface. Hence, vertical mixing in a developing mixing layer during a day may dilute $PM_{2.5}$ concentrations, while the vertical aerosol burden remains the same. Here, we investigate if accounting for the mixing layer height (MLH) also yields a better defined relation between AOD and $PM_{2.5}$ for

Cabauw.

Figure 6 shows the scatter plot between AOD and the $PM_{2.5}$ concentration multiplied by the MLH. Accounting for the actual MLH does not increase the correlation coefficient. An explanation may be that during the periods with stable fair weather conditions a residual aerosol layer is maintained above the current mixed layer as remnants of the mixed layer of the previous day, as can be identified in the LIDAR profiles in Fig. 3. In those cases a simple multiplication of $PM_{2.5}$ concentrations with the MLH would not lead to a better correlation with the AOD. We have approximated the depth of the combined mixing and residual layer by using the maximum MLH over the last 24 h. Using this approach the explained variability increases, but not significantly compared to using $PM_{2.5}$ itself. The explanation may be that the daily maximum MLH (Fig. 7) does not show a significant seasonal variation, that the use of the maximum MLH over the last 24 h dampens the variability and that the MLH varies around 1000 m during periods for which AOD data are available. An analysis with ECMWF mixing layer height (not shown) confirmed our conclusion that accounting for the mixing layer height does not improve the coefficient of determination for the AOD-$PM_{2.5}$ relation for the time series concerned in this study.

3.4.2 Meteorological conditions

The air pollution conditions as well as favourable conditions for satellite retrievals over the Netherlands depend on the large scale meteorological situation. These conditions are normally associated with easterly and southerly winds bringing continental air masses to the Netherlands. We have addressed the origin of the air masses and the meteorological conditions by using the classification scheme for synoptic situations from the German Weather Service (Hess and Brezowsky, 1977). This classification system uses 4 main regimes and 29 different subclasses. This meteorological classification yields a framework to address the air mass origin. We address the influence of the air mass origin through the 4 main regimes, as the number of occasions within each of the sub-groups is generally small.

ACPD

8, 17939–17986, 2008

Figure 8 shows the variation of $PM_{2.5}$ with AOD as function of air mass origin. In the Netherlands the most frequent air mass origin is from the west. In contrast, valid AOD measurements are scarce for this wind direction, because it is mostly associated with cloudy skies (Kusmierczyk-Michulec et al., 2007). Moreover, the data do not indicate a positively defined relation between AOD and $PM_{2.5}$. Northerly wind conditions are mostly associated with clean conditions characterised by AOD lower than 0.1 and $PM_{2.5}$ lower than 10 $\mu g/m^3$. The classification confirms that high AOD and $PM_{2.5}$ levels are associated with continental air masses arriving from the south, southeast and east. The relations between AOD and $PM_{2.5}$ for these continental situations are almost identical.

Although we have identified that the data with an air mass origin from the west do not show a positively defined relation between AOD and $PM_{2.5}$, the low number of data do not impact the results presented above. The number of data for many synoptic situations is too low to provide a basis for a statistical analysis. For such an analysis a longer time series is needed and we further neglect the air mass origin as an explanatory variable.

3.4.3 Time of day

While the ground-based measurements of AOD and $PM_{2.5}$ are obtained throughout the day, satellite observations of AOD are restricted to “snap-shots” on just a few instances during the day. To optimally apply a relation between AOD and $PM_{2.5}$ to AOD measurements of satellites, we have investigated whether the AOD-$PM_{2.5}$ relation changes when we limit the data to the time window in which the MODIS instruments pass over our site. MODIS/TERRA and MODIS/AQUA have their overpasses in the late morning and early afternoon, respectively. Here, we gradually reduce the dataset from all available observations to only observations obtained between 12:00–14:00 UTC and assess the AOD-$PM_{2.5}$ relationship.

The effect of constraining the time window is illustrated in Fig. 9 for the period between 11:00 and 15:00 UTC. Obviously, an overall reduction of available data points is

ACPD

8, 17939–17986, 2008

obtained. Also, we observe that a high percentage of the points on the edges of the data cloud are data points associated with early morning or late afternoon measurements. This is especially true for the points with low $PM_{2.5}$ and moderately high AOD values. The relations between AOD and $PM_{2.5}$ as well as the explained variability are presented in Table 5. Strikingly, the explained variability increases when we confine the time window towards midday. Also, the slope of the fit goes up significantly while the cut-off value decreases simultaneously. Therefore, we have investigated the influence of forcing the relation through zero. These fits yield slopes between 107 and 127, i.e. a more moderate increase in slope. By forcing the fit through zero the explained variability is slightly, but insignificantly, lower (<1%). Altogether, the fits that are forced through zero show a variability of less than 10% around the central value, hence, a more stable relationship between AOD and $PM_{2.5}$ than in case of a two-parameter fit allowing for a non-zero cut-off value.

Several factors related to the viewing geometry as a sun photometer is pointed directly at the sun may explain the increase in the explained variability when confining the data towards mid-day. During conditions with valid AOD retrievals the mixing layer height during midday is generally well mixed, without residual layers present. At higher solar zenith angles (low sun) the observed atmospheric path is longer and the AOD may be influenced to a larger extend by horizontal gradients in aerosol properties or atmospheric conditions. Therefore, correlation in the AOD-$PM_{2.5}$ relationship is expected to be higher under small solar-zenith angles. Finally, cloud screening using the LIDAR is probably more accurate during midday as the LIDAR profiles the atmosphere directly above the site. Under large solar zenith angles the observed part of the sky will be rather different between sun photometer and lidar. Again, better similarity is obtained under small solar zenith angles.

3.4.4 Synthesis

In this section we have established the relation between AERONET AOD and ground level $PM_{2.5}$ concentration for Cabauw. Inclusion of the mixing layer depth did not significantly improve the explained variation of the fits between AOD and $PM_{2.5}$ for the time period considered, and was therefore not used to describe the relation between AOD and $PM_{2.5}$. Moreover, retrieving the mixing layer height for large areas and combine those with satellite data (in near real time) complicates the use of such a relation. Considering that we found an increase of the correlation coefficient towards using measurement around midday we arrive at the relationship for the central time window in which the satellites that we use have their overpasses. Hence, we use the relation for the data between 11:00 and 15:00 UTC (with $PM_{2.5}$ in μg/m^3):

$PM_{2.5}$=124.5 AOD−0.34

The choice for this relation is somewhat arbitrary. Using a relation of $PM_{2.5}$=120*AOD may be as good as all determined relations yield results within 10% of this simple relation.

4 Application to MODIS data

We have used the sun photometer data to make a first assessment of the quality of the MODIS collection 5 data for the Netherlands. For this purpose, we compare co-located data within one hour of the satellite overpass in Fig. 10a. The MODIS AOD data show a very good temporal correlation explaining 80% of the variability measured from the ground. The MODIS data are slightly lower than those obtained by the sun photometer. The slope of the regression between the data is very close to 1, indicating that the underestimation is systematically about 0.05.

The validation is by definition biased to situations where both the satellite retrieval and the AERONET cloud screening identifies a cloud free situation. Situations in which only one of the two retrievals identifies a cloudy situation are not taken into account. Therefore, we have assessed the number of MODIS retrievals over Cabauw, which do have a satellite AOD value but miss an AERONET retrieval. In this manner, we determine the number of observations that could erroneously be identified as cloud-free in the cloud detection procedure of MODIS. Only 7 out of the 57 retrievals over Cabauw are not paired to an AERONET L1.5 value. Also, 14 retrievals are present where the lidar indicates that there may be cloud contamination in the sun photometer data. However, the scatter plot shows that these retrievals do not negatively impact the validation results. Hence, it may be that clouds occur in the line of sight between the sun and CIMEL, whereas more than 12 pixels above and around Cabauw were identified to be cloud-free, which allows MODIS retrieval. Furthermore, our lidar cloud screening is not perfect and this analysis may highlight the occasions where our additional cloud screening is too strict.

In Fig. 10b we show the variability of $PM_{2.5}$ as function of MODIS AOD. For MODIS we find that $PM_{2.5}$ is 120 times the AOD plus 5.1 $\mu g/m^3$. The scatter is reasonably large but the fit explains 52% of the variability in $PM_{2.5}$. The relation for the MODIS AOD compares surprisingly well with the relation determined with sun photometer data. This is especially the case considering that the slope is within the determined range with the sun photometer and that the 0.05 bias in MODIS AOD yields a cut off of 5.1 $\mu g/m^3$, where about 0.05*120=6.0 $\mu g/m^3$ is ideally expected.

To derive a first estimate of the $PM_{2.5}$ concentration field over the Netherlands based on MODIS data only, we have applied the AOD-$PM_{2.5}$ relation to the annual composite map of MODIS AOD (see Fig. 11a). MODIS AOD in the central part of the Netherlands is about 0.2–0.25. The MODIS data show high AOD values over the Ruhr area and Northern France. Minima are detected over hilly forest regions in Belgium and Germany, e.g. the Ardennes. Along the coastal area of The Netherlands, unrealistically high AOD values are observed for MODIS. At land/water boundaries, application of the land algorithm to patches of sea is likely to lead to too high AOD values (Chu et al., 2002). Furthermore, suspended sediments in shallow water may give rise to high AOD retrievals (Robles Gonzalez et al., 2000; Chu et al., 2002; Ichoku et al., 2005). This hampers the interpretation of the spatial distribution of satellite based AOD over many parts of the Netherlands, as inland water bodies (rivers, lakes) can also give rise to similar measurement artefacts. Hence, we have masked all cells in which the surface waters cover more than 10% of the 10×10 km^2 grid. In this way we also exclude the North Sea, where local sea spray emissions may significantly contribute to the AOD, which is not accounted for in the relation between AOD and $PM_{2.5}$ determined at Cabauw. In Fig. 11b we show our first estimate of the $PM_{2.5}$ distribution based on MODIS AOD in combination with the established AOD-$PM_{2.5}$ relation from Cabauw. Over the Netherlands $PM_{2.5}$ levels between 22 and 30 $\mu g/m^3$ are estimated. Lowest $PM_{2.5}$ concentrations, slightly above 11 $\mu g/m^3$, are mapped over the Ardennes and east of the Ruhr area. In the Ruhr area the resulting $PM_{2.5}$ levels are between 30 and 42 $\mu g/m^3$. Strikingly, highest $PM_{2.5}$ levels are mapped over south western Belgium and Northern France, in the region of Lille.

Some features of the spatial distribution within the Netherlands do not appear to be very realistic, although a thorough validation cannot be performed due to lack of well-calibrated $PM_{2.5}$ measurements for this period across the Netherlands and due to uncertainties in the emissions and modeling of $PM_{2.5}$. Nevertheless, features like the high values of $PM_{2.5}$ near the northern coast of the Netherlands appear unrealistic. This might be caused by smaller inland water bodies which have not been removed in the abovementioned procedure. This might also explain the relatively high derived PM levels in the flow area of the large rivers. On the other hand, the AOD-$PM_{2.5}$ relation was established within this region and we did not find an indication of an overestimation of the AOD derived from MODIS.

5 Discussion

5.1 AOD-$PM_{2.5}$ relationship

In the literature several studies report on the relation of AOD and PM_x. We have summarized the results of several studies in Table 5. The reported relations are very different as can be deduced from the large range in slopes, cut-offs and explained variability. The slopes vary between 19 and 71. The cut-off ranges between 0 and 12, where the lower cut-offs are generally associated with a steeper slope. The relations we have derived based on the AERONET data and the relation based on the MODIS data clearly indicate the highest slope compared to the other studies. On the other hand, the explained variability is the highest of all listed studies. The major variables that may explain the variability between the reported relationships are discussed below.

The comparison of relations between AOD and $PM_{2.5}$ may be influenced by the atmospheric conditions during the study. Hence, studies that focus on longer study periods are likely to find more robust results without the influence of special conditions. We have used a 10 month data set and our findings should be confirmed based on a longer time series. Hence, continuous monitoring is mandatory. For this reason, the $PM_{2.5}$ monitoring at Cabauw will be continued as part of the Dutch Air Quality network as operated by the RIVM.

The total AOD is a function of the aerosol column burden and optical properties of the aerosol. The optical properties depend on the composition and size of the aerosols. Hence, aerosol types such as marine, remote continental or polluted continental and different mixtures of these types are expected to yield another relationship. Our study is performed for polluted continental conditions. In these cases the aerosol in the Netherlands is characterized by high levels of secondary inorganic components, especially ammonium nitrate, and carbonaceous particles. Hence, the relationship is not readily applicable to other parts of the world. Several studies report on the AOD-$PM_{2.5}$ relation over the US using a host of sites from the monitoring network IMPROVE and AirNow (e.g. Al Saadi et al., 2003; Engel-Cox et al., 2004). They report that the correlation between AOD and $PM_{2.5}$ is reasonably high in the more polluted eastern part of the country, but low in the cleaner western US. These studies provide a good example for the regional applicability of the AOD-$PM_{2.5}$ relation as both aerosol types and the climatic conditions differ in these parts of the US.

Another important parameter for the slope of the relation is the characteristic mixing layer height at a location. Given an AOD for a well mixed layer the slope of the relation is inversely proportional to the layer depth. We have shown that the scale height of this layer above Cabauw varies around 1 km without showing a significant seasonal variation. Deeper layers as expected during summer time in the US and in southern Europe would yield a considerably lower slope. In addition, in areas where the scale height is more variable and shows a strong seasonal variation, accounting for this parameter may provide a more accurate parameterization as shown by Koelemeijer et al. (2006b).

Our first analysis of the data showed a relatively large number of points with a high AOD and low $PM_{2.5}$ concentration. Using the lidar we could identify that the cloud screening of the level 1.5 data does not recognize all clouds as such. An assessment using the level 2 AERONET data learned that the final screening of the level 1.5 data in the AERONET procedure, which is partly performed by expert judgment, removes a large part of the data points we identified as suspect of cloud contamination. Moreover, this final check only removes about 10% of the data that our cloud screening did not identify and remove. Hence, after applying our lidar cloud screening to both data sets, virtually the same data set is left for use in the analysis. The consistency between the datasets provides confidence in the use of the lidar as an independent method to address the quality of the sun photometer data. We conclude that the shortcomings of v1.5 compared to v2.0 are effectively removed by our additional screening for cloud contamination using the lidar profiles. When co-located LIDAR measurements are not available we advise to use the level 2.0 data. The comparison between the use of AERONET level 1.5 and 2.0 showed that the level 2.0 data contain less combinations of low $PM_{2.5}$ and high AOD. Hence, as shown in this study the use of level 2.0 data leads to higher slopes, lower cut-offs and a higher explained variability.

The earlier studies (Engel-Cox et al., 2004, 2006; Wang and Christopher, 2003) using MODIS AOD (Table 2) have used collection 4 data. Recent studies have used the newer collection 5 data. The algorithms underlying the collection 5 data have changed drastically, causing lower AOD to be retrieved in mid-latitudes, especially during summer (Levy et al., 2007a). For stations in the Netherlands and Belgium the collection 4 data showed a positive bias of 50% (Schaap et al., 2008). For collection 5 at Cabauw we find an average bias of −25%. Hence, as MODIS AOD has about halved in the

Netherlands by the change in retrieval algorithm, this can also explain a large part of the higher $PM_{2.5}$ mass per unit AOD found in this study.

Finally, the size fraction of PM is a key issue. Using PM_{10} in stead of $PM_{2.5}$ should yield a steeper slope, assuming that the coarse fraction contributes much less to the AOD than the fine fraction. This assumption is valid in most of Europe where the $PM_{2.5}$ to PM_{10} ratio tends to be larger than 0.5 (Putaud et al., 2004). Furthermore, systematic differences between PM sampling techniques associated with both automated equipment as well as filter measurements may cause variability in the reported relations. Similarly, the use of hourly or daily mean PM measurements effects the relation. Engel-Cox et al. (2006) show that especially the explained variability becomes less when using daily mean concentrations.

In short, the relationship between AOD and PM observed in one region cannot be easily extrapolated to another region, because the aerosol sources and mixtures vary regionally. The strength of the AOD-PM_x relationship may also vary due to regional dependent meteorological factors but we have shown that the methodology used to quantify the relation is a key aspect to improve the coefficient of determination. For comparison and the assessment of the region of validity, a single approach should be tested at sites throughout Europe.

5.2 Application to MODIS data

The $PM_{2.5}$-AOD relation is derived for atmospheric conditions during which satellite retrievals are available. For the Netherlands these conditions are associated with stagnant flow or low wind speed conditions bringing polluted continental air masses to the Netherlands. As a consequence the $PM_{2.5}$ concentrations are higher compared to the long term average and are characterized by a so-called fair-weather bias. In Table 6 we assess this bias during both MODIS and AERONET retrievals. The hours for which a MODIS retrieval is available show a mean concentration of 25.3 $\mu g/m^3$. The hours with a lidar cloud screened AERONET observation shows a mean value of 28 $\mu g/m^3$. The selection of all (L1.5) AERONET observations shows a lower mean of 22.7 $\mu g/m^3$, reflecting the additional cases with low $PM_{2.5}$ and high AOD values which are removed by the LIDAR cloud screening. Compared to the mean $PM_{2.5}$ concentration of 18.2 μg/m^3 during the study period, the average $PM_{2.5}$ during valid satellite retrievals is typically 40 to 55% higher.

In this study we have used MODIS data from the new MODIS algorithm (v5.2; Levy et al., 2007). The new algorithm has been updated rigorously compared to the previous version, which was used in many earlier studies. We have shown that the new collection underestimates the AOD at Cabauw in a systematic way. The underestimation does not show a seasonal dependency. In contrast, the collection 4 data showed a positive bias of about 50%. Hence, the new data are closer to the observed values at Cabauw. More importantly, the temporal correlation between MODIS and AERONET AOD has increased at the Dutch stations. A preliminary evaluation by the developers also shows better agreement with AERONET (Levy et al., 2007a). However, we cannot extrapolate this finding. Hence, the data from the new collection still need to be evaluated in detail for other areas in Europe.

We did not have the opportunity to validate our mapping results carefully as there are no other TEOM-FDMS systems operated routinely in Dutch monitoring networks. Hence, the estimated $PM_{2.5}$ distribution is of preliminary status and the validity and utility of our proposed mapping methodology should be further investigated. For this purpose, a number of sites with the same PM-monitoring equipment, located away from the coast, should be used. The validation of the $PM_{2.5}$ fields is also hampered because different atmospheric transport models also show different spatial structures over the Netherlands, stemming from, among others, uncertainties in emissions and different treatment of atmospheric chemistry. Moreover, comparison to modeled yearly average fields is difficult as the $PM_{2.5}$-field presented here holds for conditions with southerly and easterly flows over the Netherlands and is representative for the daytime. Nevertheless, some features of the spatial distribution do not appear to be very realistic, e.g. the high values of $PM_{2.5}$ around Lille and near the northern coast of the Netherlands. This might be caused by spatially varying systematic errors that are present in the

MODIS AOD data, particularly due to unaccounted variability in surface reflectance. Because of the uncertainties in current satellite data of AOD, it is not expected that better $PM_{2.5}$ maps can be constructed for the Netherlands based on satellite data alone in the near future. This conclusion may be specific for the Netherlands while many parts of continental Europe are much less affected by the presence of mixed land/water pixels than is the case within the Netherlands. Satellite measurements of AOD have added-value regarding the temporal variation of PM and when analyzed in conjunction with or combined with both surface measurements of $PM_{2.5}$ and atmospheric transport models.

6 Conclusions

The average $PM_{2.5}$ concentration at Cabauw was 18 μg/m^3, which is high in comparison with other areas in Europe and confirms that the Netherlands are characterised by a high PM burden. A first inspection of the AERONET L1.5 AOD and $PM_{2.5}$ data at Cabauw showed a low correlation between the two properties. However, after screening for cloud contamination in the AERONET L1.5 data, the correlation improved substantially. When also constraining the dataset to data points acquired around noon, the correlation between AOD and $PM_{2.5}$ amounted to R^2=0.6 for situations with fair weather. This indicates that AOD data contain important information about the temporal evolution of $PM_{2.5}$. We had used LIDAR observations to detect residual cloud contamination in the AERONET L1.5 data. Comparison of our cloud-screend L1.5 with AERONET L2 data that became available near the end of the study showed favorable agreement.

The final relation found for Cabauw is $PM_{2.5}$=124.5*AOD−0.34 (with $PM_{2.5}$ in μg/m^3) and is valid for fair weather conditions. The relationship determined between MODIS AOD and ground level $PM_{2.5}$ at Cabauw is very similar to that based on the much larger dataset from the sun photometer data, after correcting for a systematic overestimation of the MODIS data of 0.05.

ACPD
8, 17939–17986, 2008

Title Page
Abstract Introduction
Conclusions References
Tables Figures
◀◀ ▶▶
◀ ▶
Back Close
Full Screen / Esc
Printer-friendly Version
Interactive Discussion

Spatial dependent systematic errors in the MODIS AOD data, probably in part induced by the presence of mixed land/water pixels or sediments in coastal water, and the lack of knowledge on the real $PM_{2.5}$ distribution prohibit a meaningful analysis of the spatial distribution of $PM_{2.5}$ using AOD data at the scale of the Netherlands. Satellite measurements of AOD have added-value regarding the temporal variation of PM and when analyzed in conjunction with or combined with both atmospheric transport models and surface measurements of $PM_{2.5}$.

Acknowledgements. We would like to thank W. Knap, A. Los and H. Klein Baltink (KNMI) for providing the ACPADA data and mixing layer height data. Furthermore, we acknowledge the NASA/AERONET team for data maintainance, QA/QC and distribution.

References

Al-Saadi, J., Szykman, J., Pierce, R. B., Kittaka, C., Neil, D., Chu, D. A., Remer, L., Gumley, L., Prins, E., Weinstock, L., MacDonald, C., Wayland, R., Dimmick, F., and Fishman, J.: Improving national air quality forecasts with satellite aerosol observations, B. Am. Meteorol. Soc., 86(9), 1249–1261, 2005.

Apituley, A., Van Lammeren, A., and Russchenberg, H.: High time resolution cloud measurements with lidar during CLARA, Phys. Chem. Earth, 25(2), 107–113, 2000.

Brunekreef, B. and Holgate, S. T.: Air pollution and health, Lancet, 360, 1233–1242, 2002.

Builtjes, P. J. H., ten Brink, H. M., de Leeuw, G., van Loon, M., Robles Gonzales, C., and Schaap, M.: Aerosol air quality satellite data, BCRS USP-2 report 00-33, BCRS, Delft, The Netherlands, 2001.

Collins, W. D., Rasch, P. J., Eaton, B. E., Khattatov, B. V., Lamarque, J-F., and Zender, C. S.: Simulating aerosols using a chemical transport model with assimilation of satellite aerosol retrievals: Methodology for indoex, J. Geophys. Res., 106, 7313–7336, 2001.

Chu, D. A., Kaufman, Y. J., Ichoku, C.,. Remer, L. A, Tanré, D., and Holben, B. N.: Validation of MODIS aerosol optical thickness retrieval over land, Geophys. Res. Lett., 29(12), 2-1–2-4, doi:10.1029/2001GL013205, 2002.

Chu, D. A., Kaufman, Y. J., Zibordi, G., Chern, J. D., Mao, J., Li, C., and Holben, B. N.: Global monitoring of air pollution over land from the Earth Observing System-Terra

Moderate Resolution Imaging Spectroradiometer (MODIS), J. Geophys. Res., 108, 4661, doi:10.1029/2002JD003179, 2003.
de Meij, A., Wagner, S., Gobron, N., Thunis, P., Cuvelier, C., Dentener, F., and Schaap, M.: Scale issues in aerosol modeling: a case study on chemical and optical properties over the greater Milan area (Italy), June 2001, Atmos. Res., 85, 243–267, 2007.
De Haij, M., Wauben, W., and Klein Baltink, H.: Continuous mixing layer height determination using the LD-40 ceilometer: a feasibility study, KNMI report WR-2007-01, KNMI, De Bilt, the Netherlands, 2007.
Dockery, D. W., Pope III, C. A., Xu, X., Spengler, J. D., Ware, J. H., Fay, M. E., Ferris, B. G., and Speizer, F. E.: An Association between Air Pollution and Mortality in Six US Cities, New Engl. J. Med., 329, 1753–1759, 1993.
Dubovik, O. and King, M. D.: A flexible inversion algorithm for retrieval of aerosol optical properties from Sun and sky radiance measurements, J. Geophys. Res., 105, 20 673–20 696, 2000.
Dubovik, O., Smirnov, A., Holben, B. N., King, M. D., Kaufman, Y. J., Eck, T. F., and Slutsker, I.: Accuracy assessments of aerosol optical properties retrieved from AERONET sun and sky-radiance measurements, J. Geophys. Res, 105, 9791–9806, 2000.
Dürr, B. and Philipona, R.: Automatic cloud amount detection by surface longwave downward radiation measurements. J. Geophys. Res.-Atmos., 109(5), D05201, 1–9, 2004.
Eck, T. F., Holben, B. N., Reid, J. S., Dubovik, O., Smirnov, A., O'Neill, N. T., Slutsker, I., and Kinne, S.: Wavelength dependence of the optical depth of biomass burning, urban, and desert dust aerosol, J. Geophys. Res., 104, 31 333–31 350, 1999.
EEA: Europe's environment The fourth assessment, EEA, Copenhagen, 2007.
Engel-Cox, J. A., Holloman, C. H., Coutant, B. W., and Hoff, R. M.: Qualitative and quantitative evaluation of MODIS satellite sensor data for regional and urban scale air quality, Atmos. Environ, 38, 2495–2509, 2004.
Engel-Cox, J. A., Hoff, R. M., Rogers, R., Dimmick, F., Rush, A. C., Szykman, J. J., Al-Saadi, J., Chu, D. A., and Zell, E. R.: Integrating lidar and satellite optical depth with ambient monitoring for 3-D dimensional particulate characterisation, Atmos. Environ., 40, 8056–8067, 2006.
Grover, B. D., Kleinman, M., Eatough, N. L., Eatough, D. J., Hopke, P. K., Long, R. W., Wilson, W. E., Meyer, M. B., and Ambs, J. L.: Measurement of total $PM_{2.5}$ mass (nonvolatile plus semi-volatile) with the Filter Dynamic Measurement System tapered element oscillating microbalance monitor, J. Geophys. Res.-Atmos., 110(7), D07S03, 1–9,

doi:10.1029/2004JD004995, 2005.
Gupta, P. and Christopher, S. A.: Seven year particulate matter air quality assessment from surface and satellite measurements, Atmos. Chem. Phys., 8, 3311–3324, 2008, http://www.atmos-chem-phys.net/8/3311/2008/.
Hess, P. and Brezowsky, H.: Katalog der Grosswetterlagen Europas 1881–1976, 3. verbesserte und ergänzte Aufl. Berichte des Deutschen Wetterdienstes, Offenbach am Main, Germany, 113 pp., 1977.
Holben B. N., Eck, T. F., Slutsker, I., Tanre, D., Buis, J. P. Setzer, A., Vermote, E., Reagan, J. A., Kaufman, Y. F., Nakajima, T., Lavenu, F., Jankowiak, I., and Smirnov, A.: AERONET – A Federated Instrument Network and Data Archive for Aerosol Characterisation, Remote Sens. Environ., 66, 1–16, 1998.
Holben, B. N., Tanre, D., Smirnov, A., et al.: An emerging ground-based aerosol climatology: Aerosol optical depth from AERONET, J. Geophys. Res., 106, 12 067–12 097, 2001.
Hutchison, K. D.: Applications of MODIS satellite data and products for monitoring air quality in the state of Texas, Atmos. Environ., 37, 2403–2412, 2003.
Ichoku, C., Remer, L. A., and Eck, T. F.: Quantitative evaluation and intercomparison of morning and afternoon Moderate Resolution Imaging Spectroradiometer (MODIS) aerosol measurements from Terra and Aqua, J. Geophys. Res., 110, D10S03, doi:10.1029/2004JD004987, 2005.
Kacenelenbogen, M., Léon, J.-F., Chiapello, I., and Tanré, D.: Characterization of aerosol pollution events in France using ground-based and POLDER-2 satellite data, Atmos. Chem. Phys., 6, 4843–4849, 2006, http://www.atmos-chem-phys.net/6/4843/2006/.
Kappos, A. D., Bruckmann, P., Eikmann, T., Englert, N., Heinrich, U. , Hoppe, P., Koch, E., Krause, G. H. M., Kreyling, W. G., Rauchfuss, K., Rombout, P., Schulz-Klemp, V., Thiel, W. R., and Wichmann, H. E.: Health effects of particles in ambient air, Int. J. Hyg. Envir. Heal., 207, 399–407, 2004.
Kaufman, Y. J. and Tanré, D.: Algorithm for Remote Sensing of Tropospheric Aerosol from MODIS, Product ID MOD04, 1998.
Klett, J. D.: Lidar inversion with variable backscatter/extinction ratios, Appl. Optics, 24, 1638–1643, 1985.
Koelemeijer, R. B. A., Schaap, M., Timmermans, R. M. A., Homan, C. D., Matthijsen, J., van de Kassteele, J., and Builtjes, P. J. H.: Mapping aerosol concentrations and optical thickness over Europe – PARMA final report, Bilthoven, the Netherlands, MNP report 555034001,

2006a.
Koelemeijer, R. B. A., Homan, C. D., and Matthijsen, J.: Comparison of spatial and temporal variations of aerosol optical thickness and particulate matter in Europe, Atmos. Environ., 40, 5304–5315, 2006b.
Kumar, N., Chu, A., and Foster, A.: An empirical relationship between $PM_{2.5}$ and aerosol optical depth in Delhi Metropolitan, Atmos. Environ., 41, 4492–4503, 2007.
Kusmierczyk-Michulec, J., De Leeuw, G., and Moerman, M. M.: Physical and optical aerosol properties at the Dutch North Sea coast based on AERONET observations, Atmos. Chem. Phys., 7, 3481–3495, 2007, http://www.atmos-chem-phys.net/7/3481/2007/.
Levy, R. C., Remer, L. A., and Dubovik, O.: Global aerosol optical properties and application to Moderate Resolution Imaging Spectroradiometer aerosol retrieval over land, J. Geophys. Res.-Atmos., 112(13), D13210, doi:10.1029/2006JD007815, 2007a.
Levy, R. C., Remer, L. A., Mattoo, S., Vermote, E. F., and Kaufman, Y. J.: Second-generation operational algorithm: Retrieval of aerosol properties over land from inversion of Moderate Resolution Imaging Spectroradiometer spectral reflectance, J. Geophys. Res.-Atmos., 112(13), D13211, doi: 10.1029/2006JD007811, 2007b.
Liu, Y., Koutrakis, P., Kahn, R., Turquety, S., and Yantosca, R. M.: Estimating fine particulate matter component concentrations and size distributions using satellite-retrieved fractional aerosol optical depth: Part 2 – A case study, Japca J. Air Waste Ma., 57(11), 1360–1369, 2007.
Mukai, S., Sano, I., Mukai, M., and Yasumoto, M.: Evaluation of air quality from space, Proceedings of SPIE – The International Society for Optical Engineering, 6745, 67451X, 2008.
Pal, S. R., Steinbrecht, W. and Carswell, A. I., et al.: Automated method for lidar determination of cloud-base height and vertical extent, Appl. Optics, 31, 1488–1494, 1992.
Pope III, C. A., Dockery, D. W., and Schwartz, J.: Review of epidemiological evidence of health effects of particulate air pollution, Inhal. Toxicol., 7, 1–18, 1995.
Pelletier, B., Santer, R., and Vidot, J.: Retrieving of particulate matter from optical measurements: A semiparametric approach, J. Geophys. Res.-Atmos., 112(6), D06208, doi:10.1029/2006JD006737, 2007.
Putaud, J., Raesa, F., Van Dingenen, R., Bruggemann, E., Facchini, M., Decesari, S., Fuzzi, S., Gehrig, R., Hueglin, C., Laj, P., Lorbeer, G., Maenhaut, W., Mihalopoulos, N., Mueller, K., Querol, X., Rodriguez, S., Schneider, J., Spindler, G., ten Brink, H., Torseth, K, and Wiedensohler, A.: A European aerosol phenomenology – 2: chemical characteristics of

particulate matter at kerbside, urban, rural and background sites in Europe, Atmos. Environ., 38, 2579–2595, 2004.

Remer, L. A., Kaufman, Y. J., Tanré, D., Mattoo, S., Chu, D. A., Martins, J. V., Li, R.-R., Ichoku, C. , Levy, R. C., Kleidman, R. G., Eck, T. F., Vermote, E., and Holben, B. N.: The MODIS Aerosol Algorithm, Products, and Validation, J. Atmos. Sci., 62, 947–973, 2005.

Robles Gonzalez, C., Veefkind, J. P., and de Leeuw, G.: Aerosol optical depth over Europe in August 1997 derived from ATSR-2 data, Geophys. Res. Lett., 27(7), 955–958, 2000.

Russchenberg, H. W. J., Bosveld, F., Swart, D., ten Brink, H., de Leeuw, G., Uijlenhoet, R., Arbesser-Rastburg, B., van der Marel, H., Ligthart, L., Boers, R., and Apituley, A.: Ground-based atmospheric remote sensing in The Netherlands; European outlook, IEICE Transactions on Communications, E88-B(6), 2252–2258, doi:10.1093/ietcom/e88-b.6.2252, 2005.

Schaap, M., Muller, K., and ten Brink, H. M.: Constructing the European aerosol nitrate concentration field from quality analysed data, Atmos. Environ., 368, 1323–1335, 2002.

Schaap, M., Timmermans, R. M. A., Koelemeijer, R. B. A., de Leeuw, G., and Builtjes, P. J. H.: Evaluation of MODIS aerosol optical thickness over Europe using sun photometer observations, Atmos. Environ., 42, 2187–2197, doi:10.1016/j.atmosenv.2007.11.044, 2008.

Smirnov, A., Holben, B. N., Eck, T. F., Dubovik, O., and Slutsker, I.: Cloud screening and quality control algorithms for the AERONET data base, Remote Sens. Environ., 73(3), 337–349, 2000.

van de Kassteele, J., Koelemeijer, R. B. A., Dekkers, A. L. M., Schaap, M., Homan, C. D., and Stein, A.: Statistical mapping of PM_{10} concentrations over Western Europe using secondary information from dispersion modeling and MODIS satellite observations, Stoch. Env. Res. Risk A., 21(2), 183–194, doi:10.1007/s00477-006-0055-4, 2006.

van Donkelaar, A., Martin, R. V., and Park, R. J.: Estimating ground-level $PM_{2.5}$ using aerosol optical thickness determined from satellite remote sensing, J. Geophys. Res., 111, D21201, doi:10.1029/2005JD006996, 2006.

Vidot, J., Santer, R., and Aznay, O.: Evaluation of the MERIS aerosol product over land with AERONET, Atmos. Chem. Phys. Discuss., 8, 3721–3759, 2008, http://www.atmos-chem-phys-discuss.net/8/3721/2008/.

Wang, J. and Christopher, S. A.: Intercomparison between satellite-derived aerosol optical thickness and $PM_{2.5}$ mass: implications for air quality studies, Geophys. Res. Lett., 30(21), 2095, doi:10.1029/2003GL018174, 2003.

Table 1. Statistical overview of AOD and $PM_{2.5}$ data obtained during the study.

	AOD	$PM_{2.5}$ ($\mu g/m^3$)
Mean	0.29	18.2
Median	0.25	13.0
N	864	3946
min	0.04	0.0
max	2.45	156.5

ACPD

8, 17939–17986, 2008

Relation between aerosol optical depth and $PM_{2.5}$ at Cabauw

M. Schaap et al.

ACPD

8, 17939–17986, 2008

Relation between aerosol optical depth and $PM_{2.5}$ at Cabauw

M. Schaap et al.

Table 2. Statistical summary of the observed AOD, without and with screening for residual clouds using the LIDAR and APCADA cloud detection methods.

	Mean AOD	Median AOD	*N*
All data	0.29	0.25	864
LIDAR	0.27	0.24	376
APCADA	0.25	0.23	493

Table 3. Statistical summary of the sun photometer AOD data for L1.5 and L2.0 for the period between 1 August 2006 and 12 April 2007.

	AOD L1.5	AOD L2.0
Mean	0.29	0.25
Median	0.25	0.22
min	0.04	0.04
max	2.45	1.62
N	613	482

Table 4. Comparison of the number of observations in the two AERONET data sets (L1.5 and L2.0) as function of the number of LIDAR profiles per hour in which clouds were detected.

LIDAR cloud count	Number of observations L1.5	Number of observations L2.0	Data Reduction (%)
0	103	92	11
1	50	48	4
2	47	40	15
3	36	34	6
4	37	34	8
5	33	28	15
6	40	33	18
7	47	41	13
8	40	32	20
9	35	29	17
10	47	29	38
11	34	17	50
12	59	20	66

ACPD

8, 17939–17986, 2008

Relation between aerosol optical depth and $PM_{2.5}$ at Cabauw

M. Schaap et al.

Table 5. AOD-$PM_{2.5}$ relations and their explained variability as function of the time interval during the day.

Time window	$PM_{2.5}$=a*AOD+b		R^2	$PM_{2.5}$=a*AOD	R^2
	a	b		a	
0–24	97.5	2.93	0.40	107.3	0.40
9–17	111.7	0.55	0.50	113.0	0.50
10–16	106.8	0.96	0.47	110.2	0.47
11–15	124.5	−0.34	0.57	123.3	0.57
12–14	156.1	−6.92	0.72	127.8	0.71

ACPD

8, 17939–17986, 2008

Relation between aerosol optical depth and $PM_{2.5}$ at Cabauw

M. Schaap et al.

Table 6. Overview of reported AOD-PM_x relations reported in literature. For each study the fit coefficients *a* and *b*, the number of data points as well as the explained variability (R^2) are given. Furthermore, the PM quantity as well as the AOD data source are specified.

Location	PM_x	*a*	*b*	R^2	*N*	AOD	reference
Italy	PM_{10}	55	8	0.6	29	AERONET[1.5]	Chu et al. (2003)
France	PM_{10}	–	–	0.27	724	AERONET[1.5]	Pelletier et al. (2007)
France	PM_{10}	–	–	0.76	724	AERONET[1.5]	Pelletier et al. (2007)
France	$PM_{2.5}$	26	12	0.30	1974	POLDER	Kacenelenbogen et al. (2006)
US	$PM_{2.5}$	22	6	0.40	14 000	MODIS[4]	Engel-Cox et al. (2004)
US	$PM_{2.5}$	31	5	0.42	19	MODIS[4]	Engel-Cox et al. (2006)
US	$PM_{2.5}$	71	–	0.49	1095	MODIS[4]	Wang and Christopher (2003)
US	$PM_{2.5}$	29	9	0.37	1092	MODIS[5]	Gupta and Christopher (2008)

ACPD

8, 17939–17986, 2008

Relation between aerosol optical depth and $PM_{2.5}$ at Cabauw

M. Schaap et al.

Table 7. Comparison of the average $PM_{2.5}$ concentration ($\mu g/m^3$) during the whole study period and that during those hours with AOD observations.

	$PM_{2.5}$	Average $PM_{2.5}$ level associated with AOD measurements		
	TEOM-FDMS	MODIS	AERONET LIDAR	AERONET all data
Average	18.2	25.3	28.0	22.7
N	3946	35	226	464

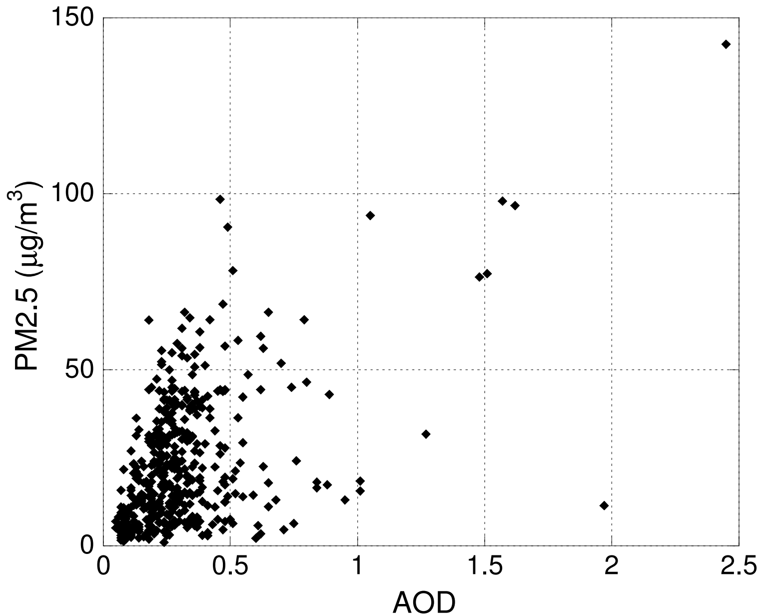

Fig. 1. Ground level $PM_{2.5}$ as function of sun photometer AOD (L1.5).

ACPD

8, 17939–17986, 2008

Relation between aerosol optical depth and $PM_{2.5}$ at Cabauw

M. Schaap et al.

Title Page
Abstract
Introduction
Conclusions
References
Tables
Figures
◀▌
▶▌
◀
▶
Back
Close
Full Screen / Esc
Printer-friendly Version
Interactive Discussion

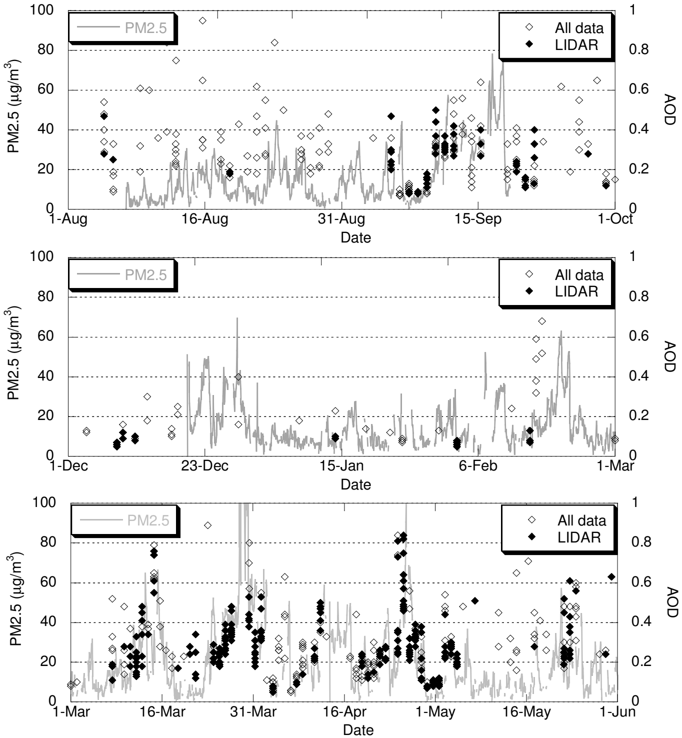

Fig. 2. Time series for $PM_{2.5}$ and AOD for the period August–September (upper panel), December–February (middle panel) and March–May (lower panel). The AERONET L1.5 AOD data are differentiated between data that did (filled diamond) and did not (open diamonds) pass our additional cloud screening based on the LIDAR profiles.

ACPD
8, 17939–17986, 2008

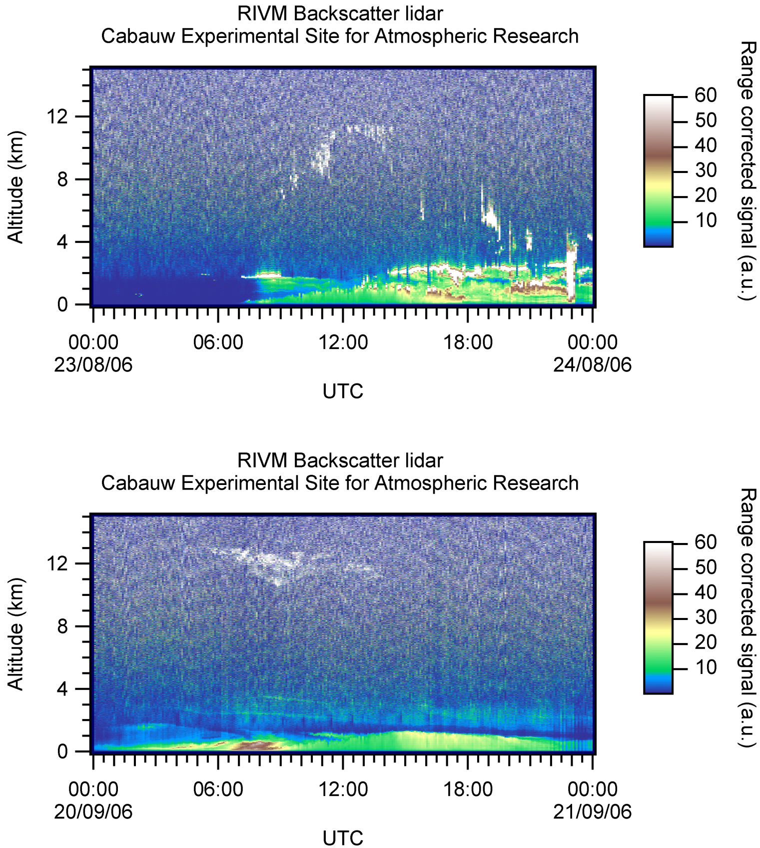

Fig. 3. Colour coded time-height plot of LIDAR data for 23 August 2006 (upper panel) and 20 September 2006 (lower panel).

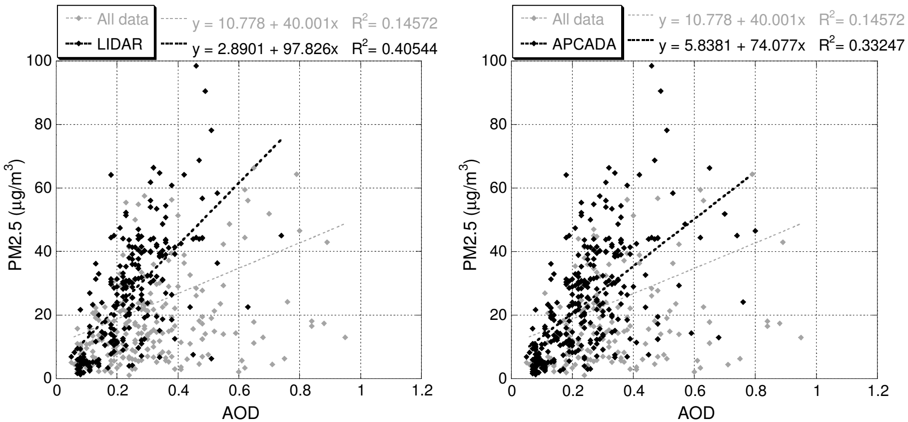

Fig. 4. Correlation between $PM_{2.5}$ and sun photometer AOD at Cabauw after screening for residual cloud contamination in the Aeronet AOD measurements based on the LIDAR (left panel) and APCADA (right panel).

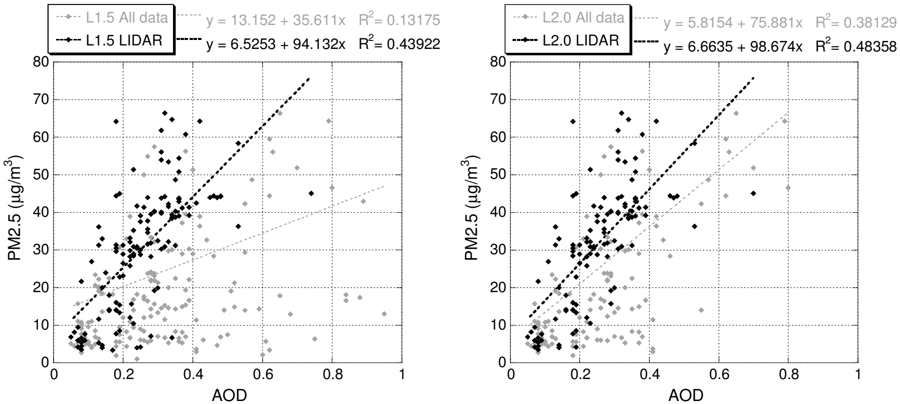

Fig. 5. Ground level $PM_{2.5}$ concentration as function of AOD for L1.5 (left) and L2.0 (right) for all data (grey) and the data that passed the LIDAR cloud screening (black). Data represent the period between 1 August 2006 and 12 April 2007.

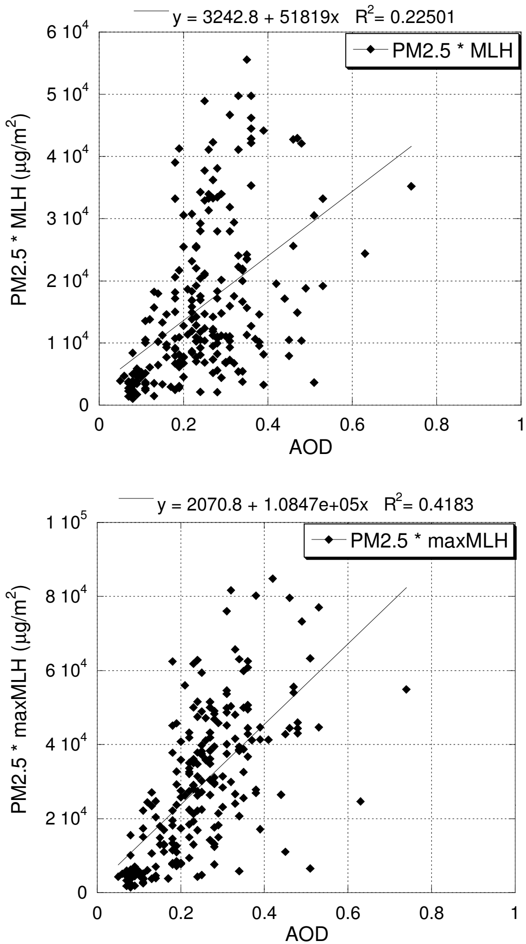

Fig. 6. The vertical aerosol burden as function of AOD. The burden is calculated using the actual (left) and 24 h maximum (right) mixing layer height (MLH).

ACPD

8, 17939–17986, 2008

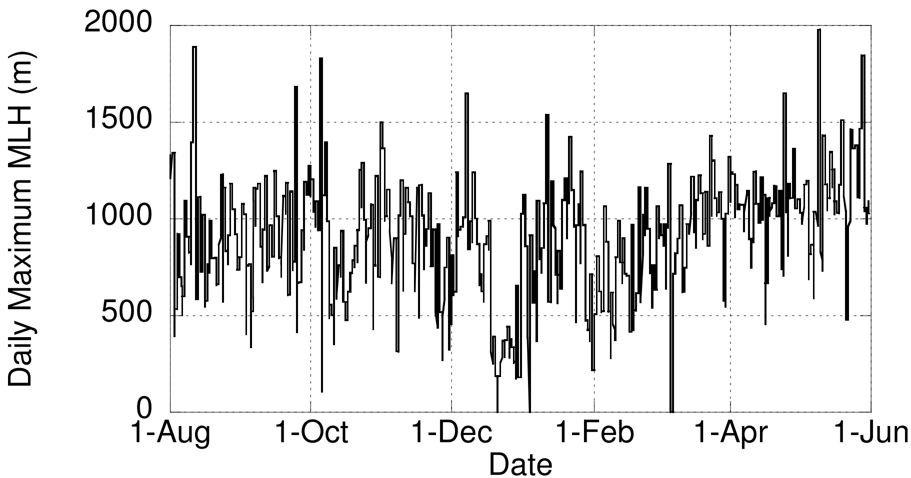

Fig. 7. The variability of the daily maximum mixing layer height (m) during the study period.

ACPD

8, 17939–17986, 2008

Relation between aerosol optical depth and $PM_{2.5}$ at Cabauw

M. Schaap et al.

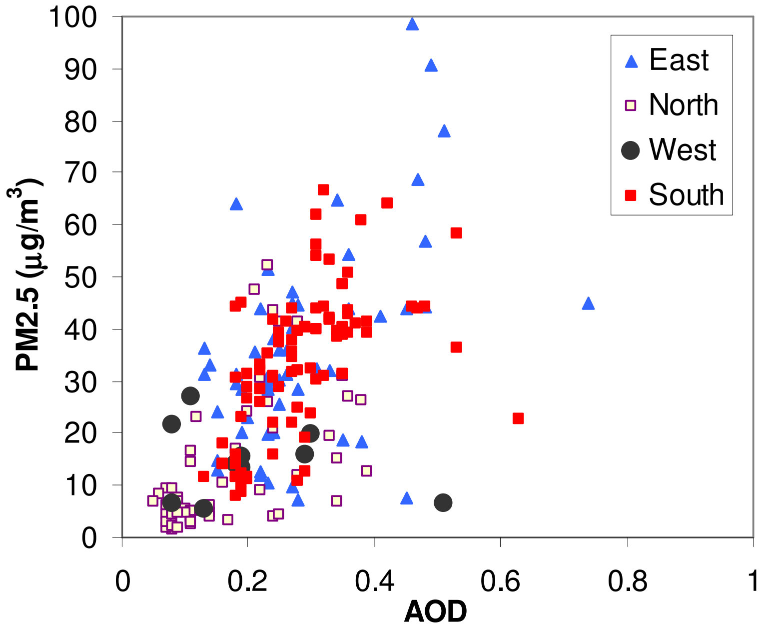

Fig. 8. The variation of $PM_{2.5}$ with AOD as function of air mass origin.

ACPD

8, 17939–17986, 2008

Relation between aerosol optical depth and $PM_{2.5}$ at Cabauw

M. Schaap et al.

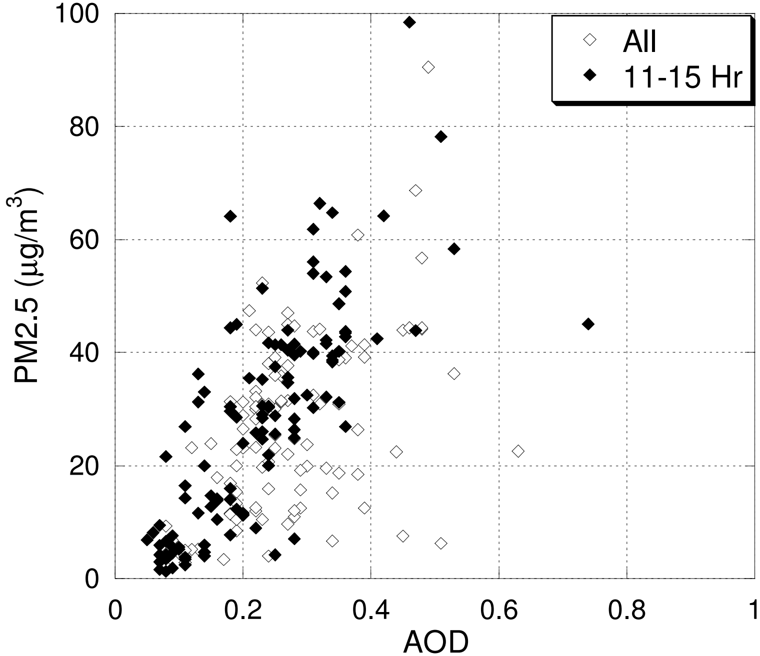

Fig. 9. The variation of $PM_{2.5}$ with AOD for all data and those between 11:00 a.m. and 15:00 p.m. hours.

ACPD
8, 17939–17986, 2008

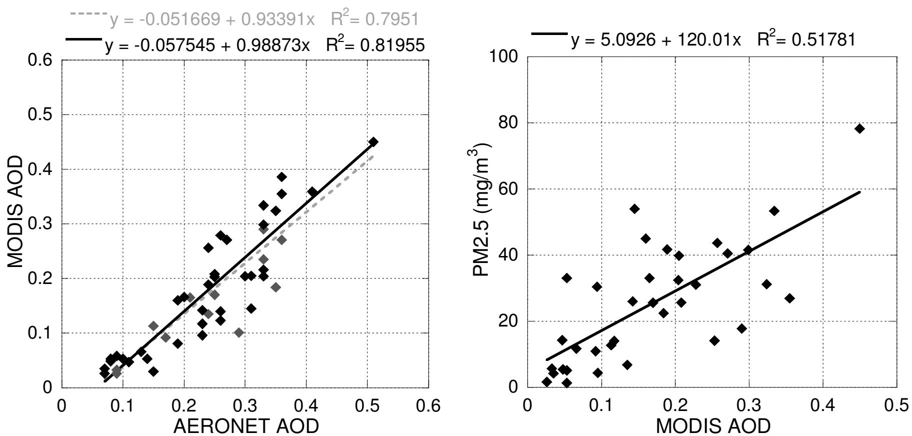

Fig. 10. (a) Validation of MODIS (left) against AERONET at Cabauw. Grey diamonds show all data, data pertaining to situations where the LIDAR indicates clear sky conditions are shown in black. **(b)** The measured $PM_{2.5}$ concentration as function of MODIS AOD.

ACPD

8, 17939–17986, 2008

Relation between aerosol optical depth and $PM_{2.5}$ at Cabauw

M. Schaap et al.

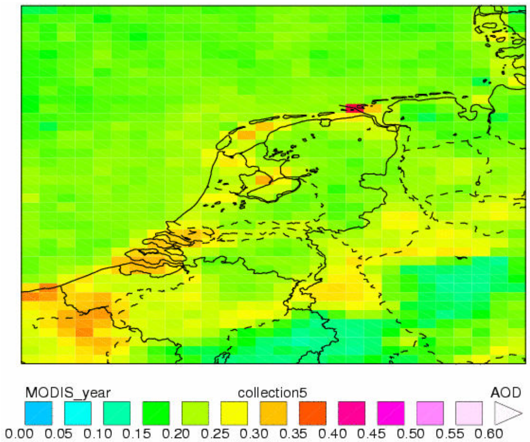

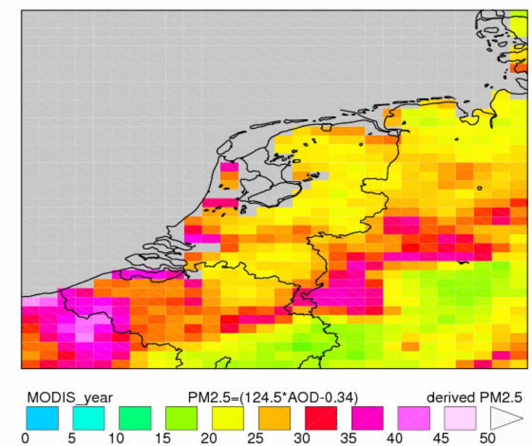

Fig. 11. **(a)** AOD composite map MODIS and **(b)** estimated $PM_{2.5}$ distribution ($\mu g/m^3$) over the Netherlands and its direct surrounding during situations with predominantly easterly and southerly flow.